Agreement of Experiment and Theory on the Single Ionization of Helium by Fast Proton Impact

H. Gassert,[1] O. Chuluunbaatar,[2,3] M. Waitz,[1] F. Trinter,[1] H.-K. Kim,[1] T. Bauer,[1] A. Laucke,[1] Ch. Müller,[1] J. Voigtsberger,[1] M. Weller,[1] J. Rist,[1] M. Pitzer,[1] S. Zeller,[1] T. Jahnke,[1] L. Ph. H. Schmidt,[1] J. B. Williams,[4] S. A. Zaytsev,[5] A. A. Bulychev,[2] K. A. Kouzakov,[6] H. Schmidt-Böcking,[1] R. Dörner,[1] Yu. V. Popov,[2,7] and M. S. Schöffler[1,*]

[1]*Institut für Kernphysik, Universität Frankfurt, Max-von-Laue-Straße 1, 60438 Frankfurt, Germany*
[2]*Joint Institute for Nuclear Research, Dubna, Moscow region 141980, Russia*
[3]*Institute of Mathematics, National University of Mongolia, 210646 Ulaanbaatar, Mongolia*
[4]*Department of Physics, University of Nevada, Reno, Nevada 89557, USA*
[5]*Department of Physics, Pacific State University, Tikhookeanskaya 136, Khabarovsk 680035, Russia*
[6]*Faculty of Physics, Lomonosov Moscow State University, Moscow 119991, Russia*
[7]*Skobeltsyn Institute of Nuclear Physics, Lomonosov Moscow State University, Moscow 119991, Russia*

(Received 4 September 2015; published 17 February 2016)

Even though the study of ion-atom collisions is a mature field of atomic physics, large discrepancies between experiment and theoretical calculations are still common. Here we present experimental results with high momentum resolution on the single ionization of helium induced by 1-MeV protons, and we compare these to theoretical calculations. The overall agreement is strikingly good, and even the first Born approximation yields good agreement between theory and experiment. This has been expected for several decades, but so far has not been accomplished. The influence of projectile coherence effects on the measured data is briefly discussed in terms of an ongoing dispute on the existence of nodal structures in the electron angular emission distributions.

DOI: 10.1103/PhysRevLett.116.073201

The ionization dynamics of atoms and molecules have been subject to investigation through the use of all kinds of ionizing projectiles. Though comparably young, fields such as the study of ionization induced by synchrotron light and lasers (and even electrons) show increasingly better agreement between experiment and theory. However, for the study of ion-atom collisions (the most mature of these fields), theory and experiment continue to show large unexplained discrepancies.

Such disagreement between the most advanced theories and experiments are particularly surprising in a regime where perturbation theory should work best, i.e., for collisions in which both the projectiles are fast compared to electron orbital velocities and the projectile charges are small; with increasing projectile velocity and decreasing perturbations, fewer terms of the Born series have to be taken into account for an appropriate description. For very fast projectiles, when the interaction times can be less than an attosecond, it has long been expected that even the first Born approximation should match the experiments perfectly. The regions in phase space most sensitive to the deficiencies of theoretical predictions are those where the amplitudes of the dominant ionization mechanism vanish. This leads to nodes in the predicted electron angular distributions. In these cases, many delicate mechanisms of interaction can manifest themselves. These can include contributions from higher-order terms in the Born series, with prominent examples being the turn-up effect in $(e, 2e)$ electron momentum spectroscopy of atoms [1], effects of the photon momentum in $(\gamma, 2e)$ reactions [2,3], and the dipole Cooper minimum in photoionization [4,5].

The experimental results of Schulz *et al.* published about a decade ago [6] are another example of this kind; indeed, since their publication, an avalanche of discussions has been launched [7–9]. We briefly review that experiment: A helium atom was singly ionized by a 100- MeV/u C^{6+} projectile. The momentum transfer q was fixed at 0.75 a.u. and the continuum electron energy at 6.5 eV. For these collision conditions, a double-lobe structure had been expected, involving a so-called binary and recoil peak with a distinct node between them. The three-dimensional emission pattern of the electron, however, showed a node only in the plane spanned by the momentum transfer and the projectile momentum. In this collision plane, experiment and theory agreed quite well. In the plane perpendicular to the momentum transfer, the expected node was filled and theory and experiment showed severe disagreement. While even the most advanced theories to date still predict a node [10–13], further experiments showed a similar behavior of a (partly) filled node [14–16]. The authors of [13,17] suggested that the origin of the discrepancies observed in the Schulz *et al.* experiment was insufficient momentum resolution; this was later refuted by Schulz *et al.* [18]. Thus, the question remains

whether this disagreement between theory and experiment is due to fundamental reasons that indicate a general problem in the field of ion-atom collisions. The present Letter attempts to shed light onto this subject by presenting the results of an analogous experiment performed with 1-MeV protons at a similar perturbation strength of $Z_p/v_p = 0.16$ a.u. (as compared to 0.1 a.u. in [6]). With our experimental setup, we achieved the highest resolution ever reported in such an ionizing ion-atom collision; this allows us to definitely rule out possible experimental sources for a disagreement between theory and experiment and also to provide a benchmark data set for future calculations in this field. In the following, we present the experimental apparatus and the calibrations we performed in more detail, as this seems to be necessary given the ongoing dispute on the influence of the experimental resolution on previous results. Atomic units are used throughout.

Experiment.—The experiment was performed at the Institut für Kernphysik at the University of Frankfurt using a Van de Graaff accelerator and the well-established cold target recoil ion momentum spectroscopy technique to measure the momentum vectors of all charged fragments created in the reaction [19] in coincidence. A 1-MeV proton beam from the accelerator (defining the z direction of the laboratory coordinate frame) was collimated using a set of variable slits with an opening of 0.5×1 mm^2 ($x \times y$). At 3.8 m downstream, a second set of slits was placed, with an opening of 0.5×1.5 mm^2. An oscillating electric field ($\approx$150 V/cm), applied on a 30-cm-long set of deflector plates 1 m behind the first collimation, was used to chop the beam (for more details see [20]) into buckets of 1-ns length at a repetition rate of 2 MHz. The projectile beam was crossed at a right angle with a supersonic He gas jet (defining the y direction of the coordinate frame). The jet was created by expanding precooled (40 K) He gas with a stagnation pressure of 2 bar through a 30-μm nozzle, resulting in a speed ratio larger than 100, a target density of 2×10^{11} atoms/cm^2, and a jet diameter of 1.5 mm at the intersection region. Accordingly, a momentum resolution in the expansion direction of $\Delta K_{p,y} = 0.1$ a.u. could be achieved. Ions and electrons created in the intersection volume of the projectile and target beam are accelerated by a weak electric field (in the x direction) of $E = 6.8$ V/cm towards two position- and time-sensitive detectors. The electron arm of the spectrometer was employed in a time-focusing geometry [21] in order to increase the momentum resolution. To reduce the diminishing influence of the extended intersection volume on the experimental resolution even further, the ion side of the spectrometer was designed as a time- and space-focusing geometry (see [22–24]). More details on this setup can be found in [25,26]. The charged fragments were detected using multichannel plate detectors with delay line anodes for position readout [27]. Hexagonal anodes [28] were used with diameters of 120 mm (electrons) and 40 mm (ions), respectively. The hexagonal approach allows for an automatic correction of nonlinearity effects, resulting in a dramatic improvement of the overall linearity and local position resolution to values of 100 μm (FWHM). A weak magnetic field of 7.5 G was superimposed parallel to the electric field to guide the electrons towards the detector [29]. From the impact position on the detectors, the time of flight [TOF(He^+) = 18 μs], the spectrometer geometry, and the values of the $\vec{E}$ and $\vec{B}$ fields, the momentum vectors of the electron and the ion have been derived. While the projectile momentum vector has not been measured directly, the excellent momentum resolution of the electron and ion allows us to deduce it based on momentum conservation. As the accuracy of the angular distributions presented later is extremely sensitive to the exact calibration of the setup, we discuss this procedure in detail in the Supplemental Material [30].

Theory.—In this Letter, we mainly performed calculations within the plane-wave first Born approximation (PWFBA), i.e., when the fast proton is treated as a plane wave both in the initial and final state. The value of the momentum transfer $\vec{q} = \vec{p}_i - \vec{p}_s$ and the energy of the ionized electron E_e are rather small, namely, $q = 0.75$ a.u. and $E_e = 6.5$ eV. The law of momentum conservation

$$\vec{q} = \vec{k}_e + \vec{K}_{\mathrm{ion}} \tag{1}$$

illustrates that the velocity of the residual ion $K_{\mathrm{ion}}/(m_N + 1)$ is negligible, considering its comparably high mass ($m_N \approx 4m_p = 7344.6$ a.u.). This allows us to assume it to be at rest during the reaction and to choose it as a center of the laboratory coordinate system.

The matrix element is given by

$$T_{fi} = \sqrt{2} Z_p \int d^3R d^3r_1 d^3r_2 \Psi_f^{-*}(\vec{R}, \vec{r}_1, \vec{r}_2; \vec{p}_s, \vec{k}_e) \Phi_i(\vec{r}_1, \vec{r}_2) \times e^{i\vec{R}\cdot\vec{p}_i} \left[\frac{2}{R} - \frac{1}{|\vec{R} - \vec{r}_1|} - \frac{1}{|\vec{R} - \vec{r}_2|} \right]. \tag{2}$$

The factor $\sqrt{2}$ accounts for the identity of the electrons labeled as 1 and 2. The function Φ_i describes the He atom in its initial (ground) state, and Ψ_f^- is the wave function of the full Hamiltonian with the final boundary conditions describing the singly ionized state. The distance between the heavy particles within the model, which has an immovable nucleus, is $\vec{R}$.

The energy conservation law

$$E = \frac{p_i^2}{2m_p} + \varepsilon_0^{He} = \frac{(\vec{p}_i - \vec{q})^2}{2m_p} + \varepsilon_0^{He^+} + \frac{k_e^2}{2} + \frac{K_{\mathrm{ion}}^2}{2(m_N + 1)} \tag{3}$$

gives the longitudinal and transversal components of the momentum transfer with respect to the incident proton momentum, $q_z = (-\varepsilon_0^{He} + \varepsilon_0^{He^+} + E_e)/v_p = 0.18$ a.u. and $q_\perp \approx m_p v_p \theta_s = 0.73$ a.u., respectively, where θ_s is the scattering angle of the proton. In Eq. (3), we neglect the

$q^2/2m_p$ and $K_{\rm ion}^2/2(m_N+1)$ terms, in line with our frozen nucleus approximation.

The final state of the reaction contains three charged particles in the continuum, namely, p, e, and the He^+ ion. In general, the Dollard asymptotic conditions [35] must be taken into account in such a case. However, since the proton energy is sufficiently high, these conditions can safely be neglected.

First, we choose simple models for the initial and final state. The final-state wave function is described by $\Psi_f^-(\vec{R},\vec{r}_1,\vec{r}_2;\vec{p}_s,\vec{k}_e)=\exp(i\vec{R}\cdot\vec{p}_s)\Phi_f^-(\vec{r}_1,\vec{r}_2;\vec{k}_e)$. In turn, the final He state with one electron in the continuum $\Phi_f^-(\vec{r}_1,\vec{r}_2;\vec{k}_e)$ is treated as a product of a hydrogenlike He^+ ground-state wave function and the wave function of the ejected electron in the Coulomb field of the residual He^+ ion. The helium ground state Φ_i is presented by two trial functions: (i) a weakly correlated Roothaan-Hartree-Fock wave function [36], which we call FBA for brevity, where both the ground and final helium states are loosely correlated wave functions, and (ii) a strongly correlated wave function of Ref. [37], which we call CFBA, as here the helium ground state is described by highly correlated wave function while its single continuum final state is still a loosely correlated wave function. We also performed numerical calculations of Φ_i and Φ_f^- within the J-matrix approach [38,39], where both the ground and final state of helium are highly correlated wave functions; this is denoted by JFBA in the following.

Another model that we used for estimations is the eikonal-wave Born approximation (EWBA). The EWBA is a variant of the well-known continuum distorted wave approach; the following method of obtaining the phase factor was pointed out in [23]. Within this approximation we obtain $\Psi_f^-(\vec{R},\vec{r}_1,\vec{r}_2;\vec{p}_s,\vec{k}_e)=\exp\{i[\vec{R}\cdot\vec{p}_s-\eta f(\vec{R},\vec{r}_1,\vec{r}_2)]\}\Phi_f^-(\vec{r}_1,\vec{r}_2;\vec{k}_e)$, with

$$f(\vec{R},\vec{r}_1,\vec{r}_2)=\ln\left\{\frac{[v_p|\vec{R}-\vec{r}_1|+\vec{v}_p\cdot(\vec{R}-\vec{r}_1)][v_p|\vec{R}-\vec{r}_2|+\vec{v}_p\cdot(\vec{R}-\vec{r}_2)]}{(v_pR+\vec{v}_p\cdot\vec{R})^2}\right\}. \quad (4)$$

Here we used $v_p=p_i/m_p=6.33$ a.u., $\eta=Z_p/v_p$, $Z_p=1$, and the proton mass $m_p=1836.15$ a.u. For calculating the integral (2), we employed the method of 9D integration described in [34]. For estimations, calculations in the second Born approximation (PWSBA) were performed in addition to the PWFBA, where we used the closure approximation for the Green's function. The details can be found in [13]. Both the EWBA and PWSBA models incorporate the effect of elastic projectile-nucleus scattering, which is not accounted for within the PWFBA. These models treat the projectile-nucleus interaction fully coherently, in contrast to the incoherent elastic-scattering mechanism proposed by Schulz *et al.* [40] as an explanation of the results of the C^{6+} experiment [6]. The applicability of the coherent or incoherent approaches was discussed in [18,41].

Results and discussion.—The data are presented in a coordinate frame defined by the initial projectile propagation direction z and the momentum transfer to the projectile q. The azimuthal angle ϕ is defined around z, while the corresponding polar angle is θ. The theoretical results have been convoluted in 2D (ϕ and θ) with an angular resolution of 5°. In Fig. 1 the experimental electron angular distribution [Fig. 1(a)] and a theoretical calculation based on the PWFBA [Fig. 1(b)] are shown for a fixed electron energy of 6.5 ± 3.5 eV and a total momentum transfer of $q=0.75\pm0.25$ a.u. In Figs. 1(c) and 1(d), these angular distributions are shown in a 3D representation, where the blue arrow represents the direction of momentum transfer q and the green arrow the beam axis z. A strongly pronounced node between the forward emitted large binary and the smaller

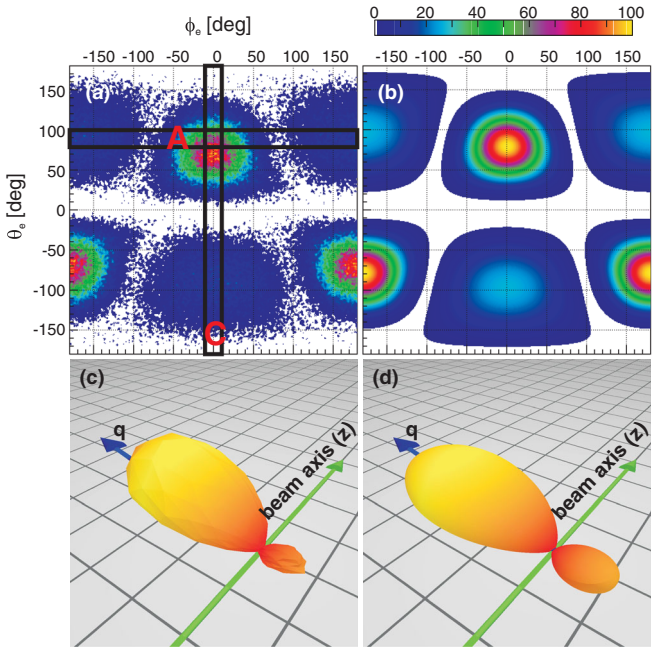

FIG. 1. Electron angular distributions for a fixed energy of $E_e=6.5\pm3.5$ eV and momentum transfer of $q=0.75\pm0.25$ a.u. (a) Experimental result and (b) theoretical distribution based on the FBA calculations. The areas marked as A and C correspond to the so-called azimuthal plane and the coplanar geometry. (c) and (d) depict 3D representations of the contour plots (a) and (b). The blue arrow indicates the direction of q and the green arrow the initial beam axis (z). The experimental data shown in (c) are mirrored at $\phi=0$ to reduce statistical fluctuations.

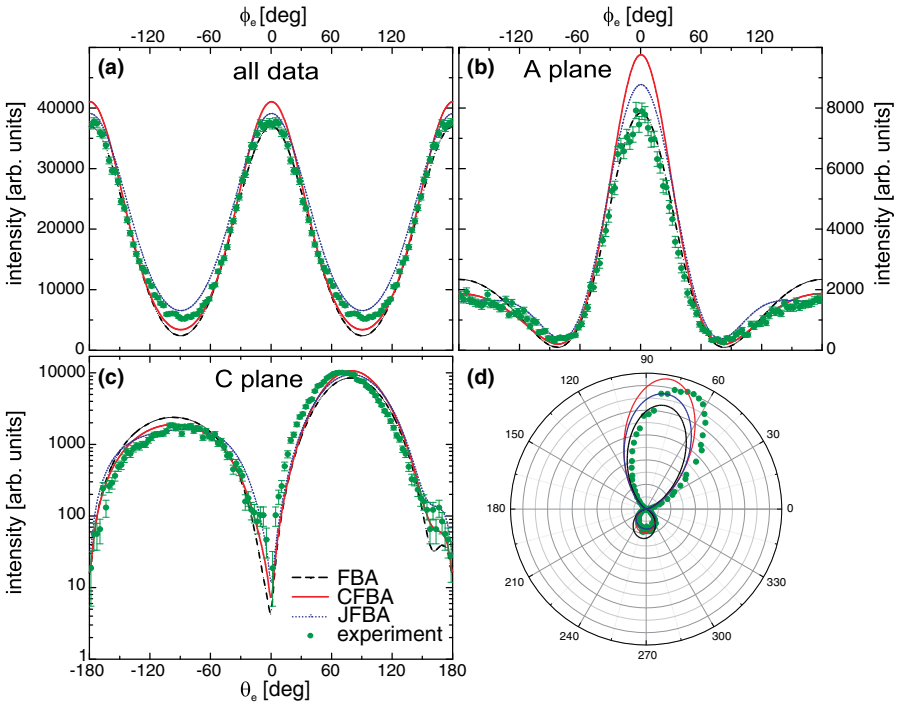

FIG. 2. Experimental (green dots) and calculated (FBA, black line; JFBA, blue line; CFBA, red line) electron angular distributions for $E_e = 6.5$ eV, $q = 0.75$ a.u. in the plane as indicated in Fig. 1(a). (a) All data; (b) azimuthal plane ($\theta_e = 90° \pm 10°$); (c),(d) coplanar geometry ($\phi_e = 0° \pm 10°$).

backward emitted recoil peak are clearly visible in theory and experiment. We emphasize that this node is not filled in any direction.

The angular distribution integrated over θ as a function of ϕ is shown in Fig. 2(a). For a quantitative comparison, the experimental data are normalized to the integral of the CFBA calculations. The FBA calculation has a slightly lower (by 7%) and the JFBA theory a slightly larger (by 8%) total cross section. Figure 2(c) shows the electron angular distribution in the coplanar geometry [the region marked as C in Figs. 1(a) and 1(b)], also known as the scattering plane. To illustrate the good agreement between experiment and theory, the data are presented on a logarithmic scale [and as a polar plot in Fig. 2(d)]. At $\theta = 0°$ the node separating the forward-pointing binary and the backward recoil peak is clearly visible and is very well matched by the experimental data. As can be seen also in the polar plot, the experimental binary lobe best matches the correlated PWFBA (CFBA) wave function [see Fig. 2(d)]. While all the first Born calculations peak at $\theta_e = 79°$, which is the direction of the momentum transfer, the experimental peak is located at $\theta_e = 73°$. We attribute this deviation to missing higher-order interaction terms, which shift the experimental binary and recoil peak forward. Indeed, our numerical estimations within the EWBA and the PWSBA for the angular domain of the binary peak show an angular shift of approximately 3° towards the experiment. Furthermore, we also find that the minimum between the recoil and binary peak is similarly pronounced for all combinations of q and E_e (not shown); only the ratios between the binary and recoil peak vary, as is well known from $(e, 2e)$ experiments [42,43].

Figure 2(b) shows the angular distribution in the azimuthal plane, marked by region A in Fig. 1(a). The simple FBA agrees best with the experimental data. It should be noted that due to the tilt of the binary lobes between theory and experiment, the direct comparison does not reflect its quality in this plane. The deviation is simply a result of the different tilts.

In conjunction with the discussion of the strong deviation between theory and experiment connected to the C^{6+} experiments of Schulz *et al.* [6], we discuss the concept of so-called projectile coherence in general and for our present data. Schulz *et al.* claim a transversal coherence of their projectile beam of $\Delta_x = 10^{-3}$ a.u. [16]. In the same publication [16] the authors claim that a coherence length of $\Delta_x = 0.25$ a.u. is sufficient to yield an incoherent beam, while $\Delta_x = 4$ a.u. corresponds to a coherent beam. For the case of a coherent beam, they observe evidence for a node between the binary and the recoil peak, which then vanishes as the beam becomes incoherent. A part of the filling of the node is attributed to the limited momentum resolution of that experiment. As our projectile beam was rectangularly collimated, a divergence of $\delta_x = 0.26$ mrad in the x direction and $\delta_y = 0.65$ mrad in the y direction was achieved. According to [16], this corresponds to a transversal coherence of 2.1 a.u. in the x direction and 0.8 a.u. in the y direction, assuming that $\Delta_{x(y)} = \delta_{x(y)}\lambda$, with λ being the de Broglie wavelength of the projectile. As the projectile beam has a different transversal coherence in

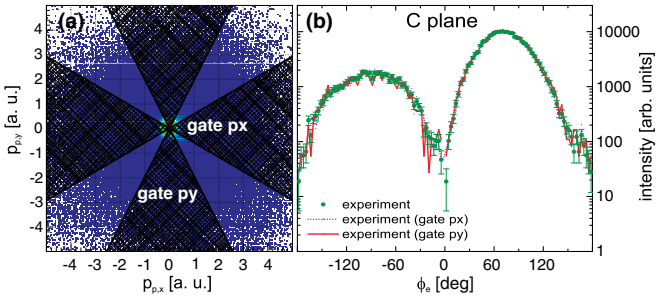

FIG. 3. (a) Projectile momenta in the laboratory xy plane, gated on $\phi_p^{\mathrm{lab}} = 0 \pm 30°$ and $\phi_p^{\mathrm{lab}} = 180 \pm 30°$ (gate px) and, respectively, $\phi_p^{\mathrm{lab}} = 90 \pm 30°$ and $\phi_p^{\mathrm{lab}} = -90 \pm 30°$ (gate py). (b) The experimental electron angular distributions in the C plane, gated and ungated.

the x and y directions in the laboratory frame, we search for its potential influence on the electron angular distribution. In Fig. 3(a), the transverse projectile momenta are shown. Two area gates, determining whether the momentum transfer occurred in the x direction or the y direction, are also depicted. Employing these gates, the electron angular distribution is plotted for the coplanar geometry in Fig. 3(b). Within the error bars, we do not observe any difference in the emission patterns obtained for gate px and gate py.

In conclusion, we have performed a high-resolution experiment on electron emissions in fast proton helium collisions. Our data are in very good agreement with the expectations from standard scattering theory with a deep node between the binary and recoil peak in all directions. We do not find any indication that the ionization process could be influenced by a possible reduced coherence of the projectile.

M. S. gratefully acknowledges financial support from the Deutsche Forschungsgemeinschaft (DFG) under Grant No. SCHO 1210/2-1. The research of three of the authors (K. A. K., Yu. V. P., and A. A. B) is supported by the Russian Foundation for Basic Research (Grant No. 14-01-00420-a). O. Ch. acknowledges support from the Hulubei-Meshcheryakov program JINR-Romania. All calculations were performed at the Moscow State University Research Computing Centre (supercomputers Lomonosov and Chebyshev) and the Joint Institute for Nuclear Research Central Information and Computer Complex. We acknowledge many years of fruitful discussion with Daniel Fischer and Michael Schulz.

*schoeffler@atom.uni-frankfurt.de

[1] C. E. Brion, Y. Zheng, J. Rolke, J. J. Neville, I. E. McCarthy, and J. Wang, J. Phys. B **31**, L223 (1998).
[2] M. Ya. Amusia, E. G. Drukarev, V. G. Gorshkov, and M. P. Kazachkov, J. Phys. B **8**, 1248 (1975).
[3] M. S. Schöffler, C. Stuck, M. Waitz, F. Trinter, T. Jahnke, U. Lenz, M. Jones, A. Belkacem, A. L. Landers, M. S. Pindzola, C. L. Cocke, J. Colgan, A. Kheifets, I. Bray, H. Schmidt-Böcking, R. Dörner, and Th. Weber, Phys. Rev. Lett. **111**, 013003 (2013).
[4] R. W. Ditchburn, Proc. R. Soc. A **117**, 486 (1928).
[5] J. W. Cooper, Phys. Rev. **128**, 681 (1962); Phys. Rev. Lett. **13**, 762 (1964).
[6] M. Schulz, R. Moshammer, D. Fischer, H. Kollmus, D. H. Madison, S. Jones, and J. Ullrich, Nature (London) **422**, 48 (2003).
[7] F. Jarai-Szabo and L. Nagy, J. Phys. B **40**, 4259 (2007).
[8] M. S. Pindzola, F. Robicheaux, and J. Colgan, Phys. Rev. A **82**, 042719 (2010).
[9] I. B. Abdurakhmanov, I. Bray, D. V. Fursa, A. S. Kadyrov, and A. T. Stelbovics, Phys. Rev. A **86**, 034701 (2012).
[10] D. Madison, M. Schulz, S. Jones, M. Foster, R. Moshammer, and J. Ullrich, J. Phys. B **35**, 3297 (2002).
[11] A. L. Harris, D. H. Madison, J. L. Peacher, M. Foster, K. Bartschat, and H. P. Saha, Phys. Rev. A **75**, 032718 (2007).
[12] M. McGovern, D. Assafrao, J. R. Mohallem, C. T. Whelan, and H. R. J. Walters, Phys. Rev. A **81**, 042704 (2010).
[13] K. A. Kouzakov, S. A. Zaytsev, Yu. V. Popov, and M. Takahashi, Phys. Rev. A **86**, 032710 (2012).
[14] D. Fischer, M. Schulz, R. Moshammer, and J. Ullrich, J. Phys. B **37**, 1103 (2004).
[15] M. Schulz, R. Moshammer, A. Voitkiv, B. Najjari, and J. Ullrich, Nucl. Instrum. Methods Phys. Res., Sect. B **235**, 296 (2005).
[16] X. Wang, K. Schneider, A. LaForge, A. Kelkar, M. Grieser, R. Moshammer, J. Ullrich, M. Schulz, and D. Fischer, J. Phys. B **45**, 211001 (2012).
[17] R. E. Olson and J. Fiol, Phys. Rev. Lett. **95**, 263203 (2005).
[18] M. Schulz, R. Moshammer, D. Fischer, and J. Ullrich, Phys. Rev. A **87**, 046701 (2013).
[19] R. Dörner, V. Mergel, O. Jagutzki, L. Spielberger, J. Ullrich, R. Moshammer, and H. Schmidt-Böcking, Phys. Rep. **330**, 95 (2000).
[20] Th. Weber, Kh. Khayyat, R. Dörner, V. Mergel, O. Jagutzki, L. Schmitt, F. Afaneh, A. Gonzales, C. L. Cocke, A. L. Landers, and H. Schmidt-Böcking, J. Phys. B **33**, 3331 (2000).
[21] W. C. Wiley and I. H. McLaren, Rev. Sci. Instrum. **26**, 1150 (1955).
[22] R. Dörner, V. Mergel, L. Spielberger, M. Achler, Kh. Khayyat, T. Vogt, H. Bräuning, O. Jagutzki, T. Weber, J. Ullrich, R. Moshammer, M. Unverzagt, W. Schmitt, H. Khemliche, M. H. Prior, C. L. Cocke, J. Feagin, R. E. Olson, and H. Schmidt-Böcking, Nucl. Instrum. Methods Phys. Res., Sect. B **124**, 225 (1997).
[23] Hong-Keun Kim, M. S. Schöffler, S. Houamer, O. Chuluunbaatar, J. N. Titze, L. Ph. H. Schmidt, T. Jahnke, H. Schmidt-Böcking, A. Galstyan, Yu. V. Popov, and R. Dörner, Phys. Rev. A **85**, 022707 (2012).
[24] M. S. Schöffler, J. N. Titze, L. Ph. H. Schmidt, T. Jahnke, O. Jagutzki, H. Schmidt-Böcking, and R. Dörner, Phys. Rev. A **80**, 042702 (2009).
[25] M. Schöffler, A. L. Godunov, C. T. Whelan, H. R. J. Walters, V. S. Schipakov, V. Mergel, R. Dörner, O. Jagutzki,

L. Ph. H. Schmidt, J. Titze, E. Weigold, and H. Schmidt-Böcking, J. Phys. B **38**, L123 (2005).
[26] M. S. Schöffler, J. Titze, L. Ph. H. Schmidt, T. Jahnke, N. Neumann, O. Jagutzki, H. Schmidt-Böcking, R. Dörner, and I. Mancev, Phys. Rev. A **79**, 064701 (2009).
[27] O. Jagutzki, J. S. Lapington, L. B. C. Worth, U. Spillman, V. Mergel, and H. Schmidt-Böcking, Nucl. Instrum. Methods Phys. Res., Sect. A **477**, 256 (2002).
[28] O. Jagutzki, A. Cerezo, A. Czasch, R. Dörner, M. Hattass, M. Huang, V. Mergel, U. Spillmann, K. Ullmann-Pfleger, Th. Weber, H. Schmidt-Böcking, and G. D. W. Smith, IEEE Trans. Nucl. Sci. **49**, 2477 (2002).
[29] R. Moshammer, M. Unverzagt, W. Schmitt, J. Ullrich, and H. Schmidt-Böcking, Nucl. Instrum. Methods Phys. Res., Sect. B **108**, 425 (1996).
[30] See Supplemental Material at http://link.aps.org/supplemental/10.1103/PhysRevLett.116.073201, which includes Refs. [23,24,31–34], for further details on the ion and electron momentum calibration.
[31] R. Ali, V. Frohne, C. L. Cocke, M. Stockli, S. Cheng, and M. L. A. Raphaelian, Phys. Rev. Lett. **69**, 2491 (1992).
[32] V. Mergel, R. Dörner, J. Ullrich, O. Jagutzki, S. Lencinas, S. Nüttgens, L. Spielberger, M. Unverzagt, C. L. Cocke, R. E. Olson, M. Schulz, U. Buck, E. Zanger, W. Theisinger, M. Isser, S. Geis, and H. Schmidt-Böcking, Phys. Rev. Lett. **74**, 2200 (1995).
[33] Th. Weber, Kh. Khayyat, R. Dorner, V. D. Rodriguez, V. Mergel, O. Jagutzki, L. Schmidt, K. A. Muller, F. Afaneh, A. Gonzalez, and H. Schmidt-Bocking, Phys. Rev. Lett. **86**, 224 (2001).
[34] M. S. Schöffler, H.-K. Kim, O. Chuluunbaatar, S. Houamer, A. G. Galstyan, J. N. Titze, T. Jahnke, L. Ph. H. Schmidt, H. Schmidt-Böcking, R. Dörner, Yu. V. Popov, and A. A. Bulychev, Phys. Rev. A **89**, 032707 (2014).
[35] J. Dollard, J. Math. Phys. (N.Y.) **5**, 729 (1964).
[36] E. Clementi and C. Roetti, At. Data Nucl. Data Tables **14**, 177 (1974).
[37] O. Chuluunbaatar, I. V. Puzynin, P. S. Vinitsky, Yu. V. Popov, K. A. Kouzakov, and C. Dal Cappello, Phys. Rev. A **74**, 014703 (2006).
[38] S. A. Zaytsev, V. A. Knyr, Yu. V. Popov, and A. Lahmam-Bennani, Phys. Rev. A **75**, 022718 (2007).
[39] Yu. V. Popov, S. A. Zaytsev, and S. I. Vinitsky, Phys. Part. Nucl. **42**, 683 (2011).
[40] M. Schulz, M. Dürr, B. Najjari, R. Moshammer, and J. Ullrich, Phys. Rev. A **76**, 032712 (2007).
[41] K. A. Kouzakov, S. A. Zaytsev, Yu. V. Popov, and M. Takahashi, Phys. Rev. A **87**, 046702 (2013).
[42] H. Ehrhardt, M. Schulz, T. Tekkaat, and K. Willmann, Phys. Rev. Lett. **22**, 89 (1969).
[43] M. Dürr, C. Dimopoulou, A. Dorn, B. Najjari, I. Bray, D. V. Fursa, Z. Chen, D. H. Madison, K. Bartschat, and J. Ullrich, J. Phys. B **39**, 4097 (2006).